EARTHQUAKE ENGINEERING AND STRUCTURAL DYNAMICS, VOL. 26, 193–213 (1997)

ACTIVE AND SEMI-ACTIVE CONTROL OF STRUCTURES UNDER SEISMIC EXCITATION

M. P. SINGH* AND E. E. MATHEU†

Department of Engineering Science and Mechanics, Virginia Polytechnic Institute and State University, Blacksburg, VA 24061, U.S.A.

AND

L. E. SUAREZ‡

Department of General Engineering, University of Puerto Rico, Mayaguez, PR 00681, U.S.A.

SUMMARY

Considerable effort has been devoted to develop passive and active methods for reducing structural response under seismic excitations. Passive control approaches have already found application in practice. Active control methods, on the other hand, are being vigorously examined for application to civil structures. This paper investigates the application of active and semi-active control schemes to structures subjected to seismic excitations, and it focuses on the use of the sliding-mode control approach for the development of the control algorithms. The possibility of control redundancy with respect to the number of sliding constraints is taken into account in the controller design. Several sets of numerical results are obtained for a realistic 10-storey shear building, subjected to earthquake-induced ground motions and controlled by active or semi-active control schemes. It is observed that both active and semi-active control schemes can be used to reduce the dynamic response. Active control performs very effectively in reducing the structural response, but the required control force values can be quite large to limit its practical application in the case of large and massive buildings. Active regulation of linear viscous dampers was found unnecessary for this type of structural system, as it did not induce any significantly more reduction in the response than the dampers acting passively. On the other hand, it is shown that active regulation of stiffness can be used with advantage to reduce the response.

KEY WORDS: structural control; active control; semi-active control; sliding mode control; building response; control requirements.

1. INTRODUCTION

It has been a common practice to design structures such that they can withstand the forces and accommodate the deformations that are induced during a design level seismic event. Recently, however, the attention has also focused on reducing these forces and deformations through structural control, to realize economical and safer structural designs. The structural response control methods can be broadly classified as passive and active control. In the passive control methods, one either dissipates the vibration energy in localized elements or devices called dampers, or deflects or filters out the energy from reaching the dominant modes of the structure by base isolators. These passive approaches are already finding applications in structural design practice.

The active control methods, on the other hand, reduce structural response by applying counteracting control forces externally or by creating reactive internal forces in the structure. Based on these two methods of generating control actions, the active control approaches are often categorized as (fully) active and semi-active, at least in the civil engineering community involved in structural control research. In the active

*Professor
†Graduate Student
‡Associate Professor

CCC 0098–8847/97/020193–21

Received 3 October 1995
Revised 30 July 1996

control methods, the counteracting control forces are applied externally by actuators driven by an adequate power source. The regulation of the control force is done according to an appropriate algorithm. In the semi-active control methods, on the other hand, the counteractive control forces are created by reactive devices with variable damping and/or stiffness characteristics. Although these methods are called semi-active, the regulation of the control action is as actively done in these methods as in the active control schemes, according to a suitable algorithm to achieve desired objectives. The operation of semi-active control devices usually requires a relatively small power source.

This paper investigates the application of both active and semi-active control schemes to structures subjected to seismic excitations. The sliding–mode control approach is utilized to develop the algorithms required for both control methods. The mathematical foundation of the sliding-mode approach is well documented in several books.[1–3] A number of publications[4–14] have further examined its formulation and explored its application in several areas. However, in the civil engineering community this is a relatively newer topic, and to the writers' knowledge, the first significant application of this approach to civil structures is due to Yang *et al.*[8] In this paper, we take a fresh look at the approach and present some new analytical developments with a somewhat different perspective, focusing on the specific aspects of seismic response control of structures. Several sets of numerical results are presented to evaluate the application of active and semi-active control schemes to civil structures.

2. ANALYTICAL FORMULATION

The equations of motion of an n_f-degree-of-freedom linear building system subjected to seismic excitation $\ddot{x}_g(t)$ and control actions $\mathbf{u}$ can be written as

$$\mathbf{M}\ddot{\mathbf{z}} + \mathbf{C}\dot{\mathbf{z}} + \mathbf{K}\mathbf{z} = -\mathbf{M}\mathbf{r}\ddot{x}_g + \mathbf{D}\mathbf{u} \tag{1}$$

in which the $n_f \times 1$ vector $\mathbf{z}$ designates the relative displacements of each degree-of-freedom and the $n_f \times n_f$ matrices $\mathbf{M}$, $\mathbf{C}$ and $\mathbf{K}$ represent the mass, damping and stiffness matrices, respectively. The $n_f \times 1$ vector $\mathbf{r}$ denotes the influence of the ground motion on each degree of freedom. The $m_c \times 1$ vector $\mathbf{u}$ contains the control actions whose locations are identified through the matrix $\mathbf{D}$. It is assumed that $m_c \leqslant n_f$ and rank $(\mathbf{D}) = m_c$.

The state equations can be written in the standard state-space form as follows:

$$\dot{\boldsymbol{\eta}} = \mathbf{A}\boldsymbol{\eta} + \mathbf{B}\mathbf{u} + \mathbf{e}\ddot{x}_g \tag{2}$$

in which the $n \times 1$ state vector $\boldsymbol{\eta}$, with $n = 2n_f$, is defined as

$$\boldsymbol{\eta} = \begin{Bmatrix} \mathbf{z} \\ \dot{\mathbf{z}} \end{Bmatrix} \tag{3}$$

The state matrix $\mathbf{A}$, input matrix $\mathbf{B}$ and disturbance vector $\mathbf{e}$ are, respectively, given by

$$\mathbf{A} = \begin{bmatrix} \mathbf{0} & \mathbf{I}_{n_f} \\ -\mathbf{M}^{-1}\mathbf{K} & -\mathbf{M}^{-1}\mathbf{C} \end{bmatrix}, \quad \mathbf{B} = \begin{bmatrix} \mathbf{0} \\ \mathbf{M}^{-1}\mathbf{D} \end{bmatrix} \quad \text{and} \quad \mathbf{e} = \begin{Bmatrix} \mathbf{0} \\ -\mathbf{r} \end{Bmatrix} \tag{4}$$

In the state equations (2), the control actions are assumed to be caused by external forces which are directly applied to the system (e.g. through hydraulic actuators). Earlier we referred to such control schemes as active control. Later on it is shown that the equations for the semi-active control case, where the control actions are introduced by time-varying parametric changes of the structural properties (e.g. by using devices with variable stiffness and/or damping characteristics) also can be cast in a form similar to equation (2).

2.1. Sliding surface and sliding motion

The main idea of the sliding-mode control approach consists of using discontinuous control actions to enforce a set of m_s pre-defined static or dynamic relationships between the state variables. This set of

constraints, whose number is assumed to satisfy $m_s \leqslant m_c$, defines a $(n - m_s)$-dimensional manifold in the state space called the *sliding surface*. If the constraints are defined through a set of linear equations, then the sliding surface is completely defined by an $m_s \times n$ matrix $\mathbf{C}_s$ as follows:

$$\mathbf{s}(\boldsymbol{\eta}) = \mathbf{C}_s\boldsymbol{\eta} = \mathbf{0} \tag{5}$$

A restriction is imposed on the class of matrices that can be used to define a sliding surface: the admissible matrices $\mathbf{C}_s$ are those satisfying rank $(\mathbf{C}_s\mathbf{B}) = m_s$.

The matrix $\mathbf{C}_s$ must be chosen in such a way that when the motion of the system (2) is forced to satisfy equation (5), the resulting motion, termed *sliding motion*, shows desirable characteristics. Therefore, to select $\mathbf{C}_s$ it is necessary to obtain a description of this motion. In view of the constraints imposed by the sliding surface, as given by equation (5), a fewer number of variables are needed to describe this motion.

This reduced order description is realized by using an appropriate transformation of the state variables. By this transformation, we will seek a representation of the system where the control actions $\mathbf{u}$ do not explicitly appear in the equations of the sliding motion. Such representation is also commonly referred to as the regular form. The transformation required to produce this decoupling will, therefore, depend on the input matrix $\mathbf{B}$. A procedure to generate this transformation was proposed by Lukyanov and Utkin,[15] based on the work by Brandin and Razorenov.[16] A particular form of this procedure was used by Yang *et al.*[8] for the case of linear systems. Also, Dorling and Zinober[17] proposed a different approach to generate this transformation. Here we propose yet another convenient and general approach.

Consider the singular value decomposition of the input matrix $\mathbf{B}$ as follows:

$$\mathbf{B} = \mathbf{V}_1\mathbf{R}\mathbf{V}_2^{\mathrm{T}} \tag{6}$$

where $\mathbf{V}_1$ and $\mathbf{V}_2$ are $n \times n$ and $m_c \times m_c$ orthogonal matrices, respectively, and the matrix $\mathbf{R}$ has the following structure:

$$\mathbf{R} = \begin{bmatrix} \boldsymbol{\Sigma} \\ \mathbf{0} \end{bmatrix} \tag{7}$$

where $\boldsymbol{\Sigma} = \mathrm{diag}(\sigma_i)$ with $\sigma_i > 0$, $i = 1, 2, \ldots, m_c$. We use this factorization of $\mathbf{B}$ to define the following transformation:

$$\boldsymbol{\eta} = \mathbf{T}\mathbf{y} \tag{8}$$

in which $\mathbf{T}$ is an orthogonal matrix given by

$$\mathbf{T} = \mathbf{V}_1\mathbf{E}_p \tag{9}$$

where $\mathbf{E}_p$ is an $n \times n$ permutation matrix. In terms of the new variables $\mathbf{y}$, the state equations (2) and the sliding surface definition (5) now can be written as

$$\dot{\mathbf{y}} = \bar{\mathbf{A}}\mathbf{y} + \bar{\mathbf{B}}\mathbf{u} + \bar{\mathbf{e}}\ddot{x}_g \tag{10}$$

$$\mathbf{s} = \bar{\mathbf{C}}_s\mathbf{y} = \mathbf{0} \tag{11}$$

where we have introduced the following notation:

$$\bar{\mathbf{A}} = \mathbf{T}^{\mathrm{T}}\mathbf{A}\mathbf{T}, \qquad \bar{\mathbf{B}} = \mathbf{T}^{\mathrm{T}}\mathbf{B}, \qquad \bar{\mathbf{e}} = \mathbf{T}^{\mathrm{T}}\mathbf{e} \quad \text{and} \quad \bar{\mathbf{C}}_s = \mathbf{C}_s\mathbf{T} \tag{12}$$

To appreciate the effect of this transformation on the system's representation, the state vector is separated into two sets of variables, denoted $\mathbf{y}_1$ and $\mathbf{y}_2$ and with sizes $n_r = n - m_s$ and m_s, respectively. With this partitioning, Equations (10) and (11) take the form

$$\begin{Bmatrix} \dot{\mathbf{y}}_1 \\ \dot{\mathbf{y}}_2 \end{Bmatrix} = \begin{bmatrix} \bar{\mathbf{A}}_{11} & \bar{\mathbf{A}}_{12} \\ \bar{\mathbf{A}}_{21} & \bar{\mathbf{A}}_{22} \end{bmatrix} \begin{Bmatrix} \mathbf{y}_1 \\ \mathbf{y}_2 \end{Bmatrix} + \begin{bmatrix} \bar{\mathbf{B}}_{1r} \\ \bar{\mathbf{B}}_{1s} \end{bmatrix} \mathbf{u} + \begin{Bmatrix} \bar{\mathbf{e}}_1 \\ \bar{\mathbf{e}}_2 \end{Bmatrix} \ddot{x}_g \tag{13}$$

$$\mathbf{s} = \bar{\mathbf{C}}_{s1}\mathbf{y}_1 + \bar{\mathbf{C}}_{s2}\mathbf{y}_2 = \mathbf{0} \tag{14}$$

From equation (13), we realize that the effect of the transformation (8) is to generate a partition $\bar{\mathbf{B}}_{1r}$ having the following structure:

$$\bar{\mathbf{B}}_{1r} = \begin{bmatrix} \mathbf{0} \\ \bar{\mathbf{B}}_{1b} \end{bmatrix} \tag{15}$$

which shows $m_c - m_s$ rows, collected in the block $\bar{\mathbf{B}}_{1b}$, that are not identically zero. However, if there is no redundancy of control actions with respect to the number of sliding constraints, e.g. $m_c = m_s$, then the block $\bar{\mathbf{B}}_{1b}$ (and consequently the whole partition $\bar{\mathbf{B}}_{1r}$) becomes a null matrix.

The description of the sliding motion can now be obtained, following the method of equivalent control.[18] Consider that the system reaches the sliding surface at some time t_h and it is forced to stay there by some control action $\hat{\mathbf{u}}$. That is,

$$\mathbf{s} = \mathbf{0} \quad \text{and} \quad \dot{\mathbf{s}}|_{\mathbf{u}=\hat{\mathbf{u}}} = \mathbf{0} \tag{16}$$

Let us obtain the control action which enforces the second condition. By considering equations (10) and (16), we note that the control $\hat{\mathbf{u}}$ must be obtained as a solution of

$$\bar{\mathbf{C}}_s\bar{\mathbf{B}}\hat{\mathbf{u}} = -\bar{\mathbf{C}}_s\bar{\mathbf{A}}\mathbf{y} - \bar{\mathbf{C}}_s\mathbf{e}\ddot{x}_g \tag{17}$$

In the standard case, defined by $m_c = m_s$, the control $\hat{\mathbf{u}}$ can be uniquely determined from this equation. For the more general case $m_c \geqslant m_s$, it is necessary to impose some additional restrictions on the control actions. If we impose the following constraints:

$$\bar{\mathbf{B}}_{1b}\hat{\mathbf{u}} = \mathbf{0} \tag{18}$$

then the dependence of the sliding equations on the control $\hat{\mathbf{u}}$ is removed. It can be shown that with these additional constraints, we obtain a unique solution of equation (17) for the control actions $\hat{\mathbf{u}}$ as

$$\hat{\mathbf{u}} = \bar{\mathbf{u}}_{eq} + \bar{\mathbf{u}}_h \tag{19}$$

where

$$\bar{\mathbf{u}}_{eq} = -\hat{\mathbf{B}}_1^{-1}\begin{bmatrix} \mathbf{0} \\ \bar{\mathbf{C}}_s\bar{\mathbf{A}} \end{bmatrix}\mathbf{y} \quad \text{and} \quad \bar{\mathbf{u}}_h = -\hat{\mathbf{B}}_1^{-1}\begin{Bmatrix} \mathbf{0} \\ \bar{\mathbf{C}}_s\bar{\mathbf{e}} \end{Bmatrix}\ddot{x}_g \tag{20}$$

in which the $m_c \times m_c$ matrix $\hat{\mathbf{B}}_1$ is defined as follows:

$$\hat{\mathbf{B}}_1 = \begin{bmatrix} \bar{\mathbf{B}}_{1b} \\ \bar{\mathbf{B}}_{1s} \end{bmatrix} \tag{21}$$

Substituting equations (19) and (20) into equation (13), we obtain the following reduced order representation, describing the behaviour of the system under conditions (16) and (18):

$$\dot{\mathbf{y}}_1 = [\bar{\mathbf{A}}_{11} - \bar{\mathbf{A}}_{12}\bar{\mathbf{C}}_{s1}]\mathbf{y}_1 + \bar{\mathbf{e}}_1\ddot{x}_g \tag{22}$$

where it has been assumed that $\bar{\mathbf{C}}_{s2} = \mathbf{I}_{m_s}$ without any loss of generality. This equation offers a very convenient framework to define the sliding surface. The selection of the sliding surface is completed by choosing the matrix $\bar{\mathbf{C}}_{s1}$ such that we obtain some desirable characteristics for the reduced order dynamics described by equation (22). Several approaches have been proposed to obtain $\bar{\mathbf{C}}_{s1}$ and their details can be found elsewhere.[19,20] For the numerical results presented later, the selection of the sliding surface was based by the minimization of a quadratic performance index.[19]

2.2. Control system design

Having established the sliding surface, it is necessary to define m_c control actions required to force the system state to reach this surface, and then maintain it there. In the general case, as indicated previously, these actions involve some form of discontinuity with respect to the sliding surface. This is needed to alter the

structure of the system each time the state $\boldsymbol{\eta}$ tends to move away from $\mathbf{s} = \mathbf{0}$. A classical approach for the design of the sliding-mode controller is based on Lyapunov's direct method, since the objective is to guarantee that $\mathbf{s} = \mathbf{0}$ is an asymptotically stable equilibrium point.[7] This framework allows for the design not only of discontinuous but also continuous controllers.

Let us consider the following Lyapunov function candidate:

$$V = \tfrac{1}{2}\,\mathbf{s}^{\mathrm{T}}\mathbf{P}\mathbf{s} \tag{23}$$

where $\mathbf{P}$ is an $m_s \times m_s$ symmetric positive-definite constant matrix. The time derivative of this function is given by

$$\frac{\mathrm{d}}{\mathrm{d}t}(V) = \mathbf{s}^{\mathrm{T}}\mathbf{P}\bar{\mathbf{C}}_s\{\bar{\mathbf{A}}\mathbf{y} + \bar{\mathbf{e}}\ddot{x}_g\} + \mathbf{s}^{\mathrm{T}}\mathbf{P}\bar{\mathbf{C}}_s\bar{\mathbf{B}}\mathbf{u} \tag{24}$$

In order to guarantee the attractiveness of the sliding surface, the control actions must force this function to be negative. In the sequel, we investigate some possible active and semi-active controllers.

2.2.1. Active control. Let us consider first the design of an active control system. As mentioned by De Carlo *et al.*,[7] a sliding-mode controller has typically the following structure:

$$\mathbf{u} = \mathbf{u}_s + \mathbf{u}_b \tag{25}$$

The component $\mathbf{u}_s$ involves, in general, some form of constant state feedback and/or disturbance measurement, if available. On the other hand, the component $\mathbf{u}_b$ may represent some linear, non-linear or discontinuous form of state feedback. Depending on the redundancy of the control actions with respect to the number of sliding constraints, several possible controllers characterized by different components $\mathbf{u}_s$ and $\mathbf{u}_b$ can be formulated. Since the case $m_c = m_s$ has been thoroughly explored in the literature, we will briefly describe the design of some controllers for the general case $m_c \geqslant m_s$.

A possible controller is based on the component $\mathbf{u}_s$ selected as follows:

$$\mathbf{u}_s = \bar{\mathbf{u}}_{eq} + \bar{\mathbf{u}}_h \tag{26}$$

To define the component $\mathbf{u}_b$, let us consider the singular value decomposition of the matrix $\bar{\mathbf{C}}_s\bar{\mathbf{B}}$ given by

$$\bar{\mathbf{C}}_s\bar{\mathbf{B}} = \mathbf{U}_1\mathbf{G}\mathbf{U}_2^{\mathrm{T}} \tag{27}$$

where $\mathbf{U}_1$ and $\mathbf{U}_2$ are $m_s \times m_s$ and $m_c \times m_c$ orthogonal matrices, respectively, and the matrix $\mathbf{G}$ is given by

$$\mathbf{G} = [\boldsymbol{\Gamma}\ \mathbf{0}] \tag{28}$$

with $\boldsymbol{\Gamma} = \mathrm{diag}(\gamma_i)$ with $\gamma_i > 0$, $i = 1, 2, \ldots, m_s$. Using the factorization indicated in Eq. (27), we choose

$$\mathbf{u}_b = -\mathbf{U}_2 \begin{Bmatrix} \boldsymbol{\Delta}_1\ \mathrm{sgn}(\boldsymbol{\sigma}) \\ \mathbf{0} \end{Bmatrix} \tag{29}$$

where $\boldsymbol{\Delta}_1$ is a weighting matrix of the form $\boldsymbol{\Delta}_1 = \mathrm{diag}(\delta_{1i})$, with $\delta_{1i} > 0$ for $i = 1, 2, \ldots, m_s$, and the variables $\boldsymbol{\sigma}$ are defined as follows:

$$\boldsymbol{\sigma} = \mathbf{U}_1^{\mathrm{T}}\mathbf{s} \tag{30}$$

Substituting equations (26) and (29) into equation (24), and selecting $\mathbf{P} = \mathbf{I}_{m_s}$, the time derivative of the function V takes the form

$$\frac{\mathrm{d}}{\mathrm{d}t}(V) = -\boldsymbol{\sigma}^{\mathrm{T}}\boldsymbol{\Pi}_1\,\mathrm{sgn}(\boldsymbol{\sigma}) \tag{31}$$

where we have defined $\mathbf{\Pi}_1 = \mathbf{\Gamma}\mathbf{\Delta}_1$. If we define $\lambda_1 = \min\{\gamma_i \delta_{1i}\}$, we have that

$$\frac{\mathrm{d}}{\mathrm{d}t}(V) \leqslant -\lambda_1 \| \boldsymbol{\sigma} \|_1 \tag{32}$$

which is obviously negative whenever $\mathbf{s} \neq \mathbf{0}$.

A distinct advantage of discontinuous control laws generating sliding motions is their superb robustness with respect to parameter uncertainties and external disturbances. However, such discontinuous switching of the control actions can lead to a high-frequency control activity which is in general undesirable. To avoid this problem, one can use a continuous control law to approximate the robust behaviour of the classical sliding-mode controller. Several such controllers have been proposed by Slotine and Sastry,[5] Ambrosino *et al.*[21] and Burton and Zinober,[22] among others. Excellent applications of continuous sliding-mode controllers to civil structures are presented by Yang *et al.*[8–13] Many of the aforementioned control laws are based on the availability of information about the external disturbance. However, using the concepts from the theory of control of uncertain systems developed by Leitmann *et al.*, [23,24] it is still possible to develop controllers based only on bounds on the possible size of the disturbance, as shown by Corless and Leitmann,[24] Ryan and Corless[25] and Zhou and Fisher,[26] among others. In the following, we present a controller of this type for the general case $m_c \geqslant m_s$.

For this case, the component $\mathbf{u}_s$ is selected as follows:

$$\mathbf{u}_s = \bar{\mathbf{u}}_{eq} \tag{33}$$

and considering again the factorization (27), we define $\mathbf{u}_b$ as

$$\mathbf{u}_b = -\mathbf{U}_2 \begin{Bmatrix} \mathbf{\Delta}_2 \boldsymbol{\sigma} \\ \mathbf{0} \end{Bmatrix} \tag{34}$$

where $\boldsymbol{\sigma}$ is defined in (30) and $\mathbf{\Delta}_2$ is a weighting matrix of the form $\mathbf{\Delta}_2 = \mathrm{diag}(\delta_{2i})$, with $\delta_{2i} > 0$ for $i = 1, 2, \ldots, m_s$. Substituting equations (33) and (34) into equation (24), and selecting $\mathbf{P} = \mathbf{U}_1 \mathbf{U}_1^{\mathrm{T}}$, the time derivative of the function V now takes the form

$$\frac{\mathrm{d}}{\mathrm{d}t}(V) = \boldsymbol{\sigma}^{\mathrm{T}} \mathbf{U}_1^{\mathrm{T}} \boldsymbol{\mu} + \boldsymbol{\sigma}^{\mathrm{T}} \mathbf{\Pi}_2 \boldsymbol{\sigma} \tag{35}$$

where we have defined $\mathbf{\Pi}_2 = \mathbf{\Gamma}\mathbf{\Delta}_2$ and $\boldsymbol{\mu} = \bar{\mathbf{C}}_s \bar{\mathbf{e}} \ddot{x}_g$. Now, let $\ddot{x}_g^{\max}$ be a bounding value for the ground acceleration to which the structure is likely to be subjected, that is,

$$|\ddot{x}_g(t)| \leqslant \ddot{x}_g^{\max} \tag{36}$$

This value may be chosen as the maximum ground acceleration value that can be expected at the site. In terms of this expected ground motion parameter, the following inequality holds:

$$\| \boldsymbol{\mu} \|_2 \leqslant \| \mathbf{C}_s \mathbf{e} \|_2 \ddot{x}_g^{\max} = \xi_{\max} \tag{37}$$

Finally, considering equation (37) and defining $\lambda_2 = \min\{\gamma_i \delta_{2i}\}$, the time derivative of the function V can now be shown to satisfy to following inequality:

$$\frac{\mathrm{d}}{\mathrm{d}t}(V) \leqslant \left(\frac{1 - 2\lambda_2}{2} \right) \| \boldsymbol{\sigma} \|_2^2 + \tfrac{1}{2} \xi_{\max}^2 \tag{38}$$

Depending upon the choice of the design parameters in the matrix $\mathbf{\Delta}_2$, which defines λ_2, and provided that $\lambda_2 > 1/2$, the last inequality establishes a region defined by

$$\| \boldsymbol{\sigma} \|_2^2 > \frac{\xi_{\max}^2}{2\lambda_2 - 1} \tag{39}$$

where the attraction to a neighbourhood of the sliding surface is guaranteed. Note that now the control cannot guarantee the global asymptotic stability of the point $\mathbf{s} = \mathbf{0}$ but instead it assures that all trajectories will ultimately lie within a neighbourhood of that point. Notice that this is a conservative bound and in practice the system will stay in a region closer to the origin $\mathbf{s} = \mathbf{0}$ than the lower bound defined by equation (39).

2.2.2. Semi-active control. In this approach, the control actions are generated through m_c devices having variable stiffness and damping characteristics. Here we will consider a model in which variable stiffness and damping mechanisms are installed in parallel along diagonal braces that are hinged to the main structure. Each device is characterized by variable stiffness and damping coefficients k_{v_i} and c_{v_i} which we assume can be changed independently. (This assumption implies, for example, that for the case in which the variable damping action is provided through a hydraulic mechanism, we neglect the fluid compliance effect.)

We assume also that the number of such semi-active devices is at most equal to the number of degrees of freedom, that is $m_c \leqslant n_f$. For this case, the equations of motion (1) take the following form:

$$\mathbf{M}\ddot{\mathbf{z}} + [\mathbf{C} + \mathbf{C}_v]\dot{\mathbf{z}} + [\mathbf{K} + \mathbf{K}_v] = -\mathbf{M}\mathbf{r}\ddot{x}_g \tag{40}$$

in which the matrices $\mathbf{C}_v$ and $\mathbf{K}_v$ represent the contributions of the variable damping and stiffness parameters, respectively, with $\text{rank}(\mathbf{C}_v) = \text{rank}(\mathbf{K}_v) = m_c$. In state-space form, we can write the equations of motion as follows:

$$\dot{\boldsymbol{\eta}} = \mathbf{A}\boldsymbol{\eta} + \mathbf{B}_2\mathbf{v} + \mathbf{e}\ddot{x}_g \tag{41}$$

in which

$$\mathbf{B}_2 = \begin{bmatrix} \mathbf{0} \\ \mathbf{M}^{-1} \end{bmatrix} \quad \text{and} \quad \mathbf{v} = -[\mathbf{K}_v \quad \mathbf{C}_v]\boldsymbol{\eta} \tag{42}$$

To achieve a more convenient representation for the contribution of the semi-active devices, we use an $n_f \times n_f$ non-singular matrix $\mathbf{T}_c$ such that the following congruence transformations can be generated:

$$\mathbf{T}_c^T\mathbf{K}_v\mathbf{T}_c = \begin{bmatrix} \mathbf{K}_v^r & \mathbf{0} \\ \mathbf{0} & \mathbf{0} \end{bmatrix} \quad \text{and} \quad \mathbf{T}_c^T\mathbf{C}_v\mathbf{T}_c = \begin{bmatrix} \mathbf{C}_v^r & \mathbf{0} \\ \mathbf{0} & \mathbf{0} \end{bmatrix} \tag{43}$$

where $\mathbf{K}_v^r = \text{diag}(k_{v_i})$ and $\mathbf{C}_v^r = \text{diag}(c_{v_i})$, $i = 1, 2, \ldots, m_c$. We use these two reduced diagonal matrices to write the state equations in terms of the variables $\mathbf{y}$ as follows:

$$\dot{\mathbf{y}} = \bar{\mathbf{A}}\mathbf{y} + \bar{\mathbf{B}}_{2r}\mathbf{v}_r + \bar{\mathbf{e}}\ddot{x}_g \tag{44}$$

in which

$$\bar{\mathbf{B}}_{2r} = \mathbf{T}^T\begin{bmatrix} \mathbf{0} \\ \mathbf{M}^{-1} \end{bmatrix}\mathbf{L}^T, \qquad \mathbf{v}_r = -[\mathbf{K}_v^r\,\mathbf{C}_v^r]\begin{Bmatrix} \boldsymbol{\xi} \\ \dot{\boldsymbol{\xi}} \end{Bmatrix} \tag{45}$$

where the variables $\boldsymbol{\xi}$ are given by

$$\boldsymbol{\xi} = \mathbf{L}^T\mathbf{z} \tag{46}$$

and the $m_c \times n_f$ matrix $\mathbf{L}$ is defined as follows:

$$\mathbf{L} = [\mathbf{I}_{m_c} \quad \mathbf{0}]\,\mathbf{T}_c^{-1} \tag{47}$$

Considering equation (44) and selecting $\mathbf{P} = \mathbf{I}_{m_s}$ in equation (23), the time derivative of the function V is given by

$$\frac{\mathrm{d}}{\mathrm{d}t}(V) = \mathbf{s}^T\bar{\mathbf{C}}_s\{\bar{\mathbf{A}}\mathbf{y} + \bar{\mathbf{e}}\ddot{x}_g\} + \mathbf{s}^T\bar{\mathbf{C}}_s\bar{\mathbf{B}}_{2r}\mathbf{v}_r \tag{48}$$

In the case of semi-active control, the control actions cannot achieve any arbitrary value. They are constrained by the fact that the semi-active devices can only provide non-negative stiffness and damping values k_{v_i} and c_{v_i}. Therefore, although these control actions may succeed in bringing the system state towards the sliding surface, they may not be able to force the system to stay there. Therefore, because of the limited control action available in the semi-active case, $\mathbf{s}$ may not be equal to zero. Noting that $V = \frac{1}{2}\mathbf{s}^T\mathbf{s}$ provides a measure of this separation from $\mathbf{s} = \mathbf{0}$, the objective of the semi-active control is to minimize the value of this function, in order to reduce any tendency of the system state to move away from $\mathbf{s} = \mathbf{0}$. Therefore, the goal of the semi-active control system reduces to enforce the following condition:

$$\mathbf{s}^T\bar{\mathbf{C}}_s\bar{\mathbf{B}}_{2r}\mathbf{v}_r \leqslant 0 \tag{49}$$

Taking into account the structure of $\mathbf{v}_r$ in equation (45), we note that a possible way to enforce condition (49) is given by the following control law, assuming that the each semi-active device can only provide two different values of stiffness ($k_{v_i}^{min}$ and $k_{v_i}^{max}$) and damping ($c_{v_i}^{min}$ and $c_{v_i}^{max}$):

$$k_{v_i} = \tfrac{1}{2}(k_{v_i}^{max}(1 + \mathrm{sgn}(g_i\dot{\xi}_i)) + k_{v_i}^{min}(1 - \mathrm{sgn}(g_i\dot{\xi}_i))) \tag{50}$$

$$c_{v_i} = \tfrac{1}{2}(c_{v_i}^{max}(1 + \mathrm{sgn}(g_i\dot{\xi}_i)) + c_{v_i}^{min}(1 - \mathrm{sgn}(g_i\dot{\xi}_i))) \tag{51}$$

where the vector $\mathbf{g}$ is defined by

$$\mathbf{g} = \mathbf{s}^T\bar{\mathbf{C}}_s\bar{\mathbf{B}}_{2r} \tag{52}$$

The controller described by Equations (50) and (51) is essentially the same as originally proposed by Yang *et al.*[8]

3. NUMERICAL RESULTS

Since the primary focus of this work is on the control of (usually massive) civil structures subjected to seismic motions, a 10-storey shear building model subjected to recorded earthquake-induced ground motions, is considered as an example problem. The structure represents a typical medium-sized multi-storey building whose floor weights correspond to about 400 m^2 of floor area. Each storey has the same mass, stiffness and damping parameters. The structural properties and natural frequencies of this example structure are provided in Figure 1. The resulting proportional damping matrix for the structure provided a modal damping ratio of 3.1 per cent of the critical in the fundamental mode.

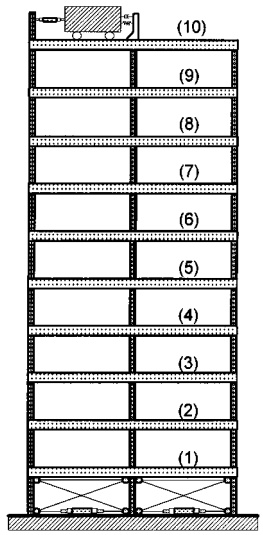

Floor Mass:
357.24 [kN.sec^2/m]

Floor Stiffness:
654.98 [MN/m]

Floor Damping:
6.15 [MN.sec/m]

	Natural Freqs. [rad/sec]
1	6.40
2	19.06
3	31.29
4	42.82
5	53.39
6	62.78
7	70.76
8	77.16
9	81.83
10	84.68

Figure 1. Schematics of the example problem: 10-storey building with active tuned mass damper and active tendons

3.1. *Active control*

To apply the control actions to the building, two different methods were considered: Force applied through (1) a system of active tendons (ATS) applied at first floor level and (2) a Tuned Mass Damper (TMD) situated on the building roof. One realizes that, depending on the aspect ratio of the building, the application of active tendon forces on higher levels would be associated with large vertical forces.

To evaluate the effectiveness of the control system for different disturbances, four different seismic events were used in the numerical simulations. In particular, the ground acceleration records obtained in (1) El Centro, 1941, (2) San Fernando, 1971, (3) Loma Prieta, 1989, and (4) Kern County, 1952 (recorded at the Hollywood basement site), earthquake events have been considered. All four records were normalized to a maximum acceleration level of 0·3 g. The ground acceleration response spectra for 3 per cent damping ratio are shown in Figure 2 for the four inputs. Also shown, along the frequency axis are the locations of the natural frequencies of the structure.

In the case of the control force applied through a tuned mass damper, the TMD was nearly tuned to the first modal frequency with a frequency ratio of 0·91. The mass of the damper was about 30 per cent of the top floor mass and the corresponding damping ratio was chosen to be about 11 per cent of the critical value. The control force was provided between the damper mass and the reaction wall (or support) on the top floor.

The continuous controller defined in equations (33) and (34) was used to define the control actions for the active tendon system and the tuned mass damper. In Figure 3, we show the time histories of the top floor displacements for the controlled and uncontrolled systems and for both methods of applying the control force. Similar results are shown in Figure 4 for the base shear force responses. These results are obtained for the El Centro ground motion. It is observed that the control actions do modify the response and reduce the peak values. In Figure 5, we show the floor acceleration response spectra for the top floor for the two cases, again compared with the uncontrolled case. It is noted that the control action does reduce the maximum floor acceleration (as represented by the response spectrum value at high frequency) as well as the peak floor response spectrum value.

From a practical standpoint, it is desirable to know what one can expect in terms of the actuator requirements to achieve such a reduction of the responses. In Figure 6, we plot the time histories of the actuator force for the tuned mass damper and active tendon systems. It is noted that the magnitude of the actuator force required in tendon control is much larger than the force required with the tuned mass damper.

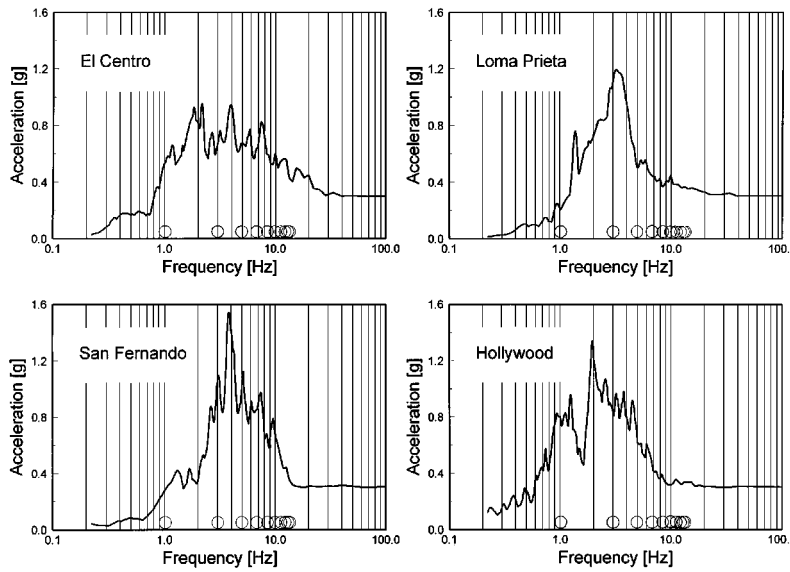

Figure 2. Acceleration response spectra for El Centro, Loma Prieta San Fernando and Hollywood ground acceleration records (all normalized to 0.3 g)

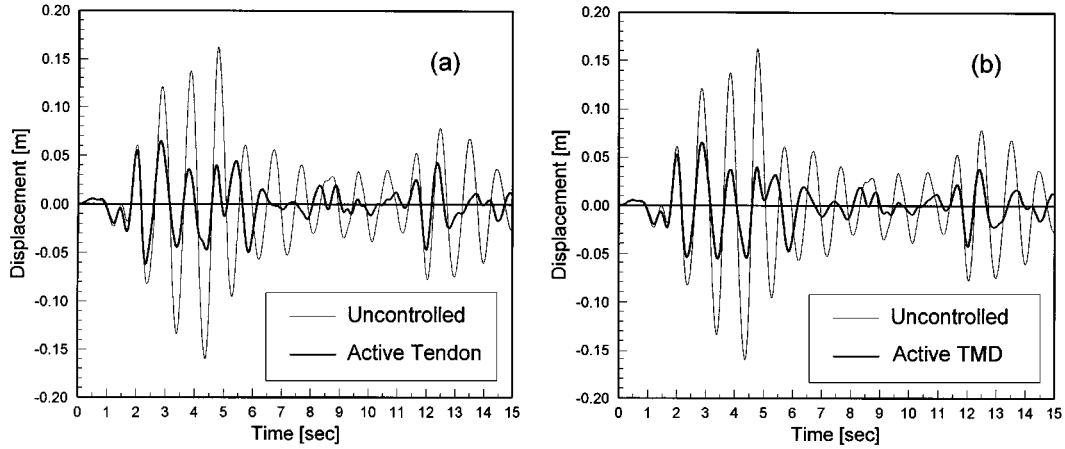

Figure 3. Uncontrolled and controlled top floor displacement: (a) active tendon control and (b) active tuned mass damper control

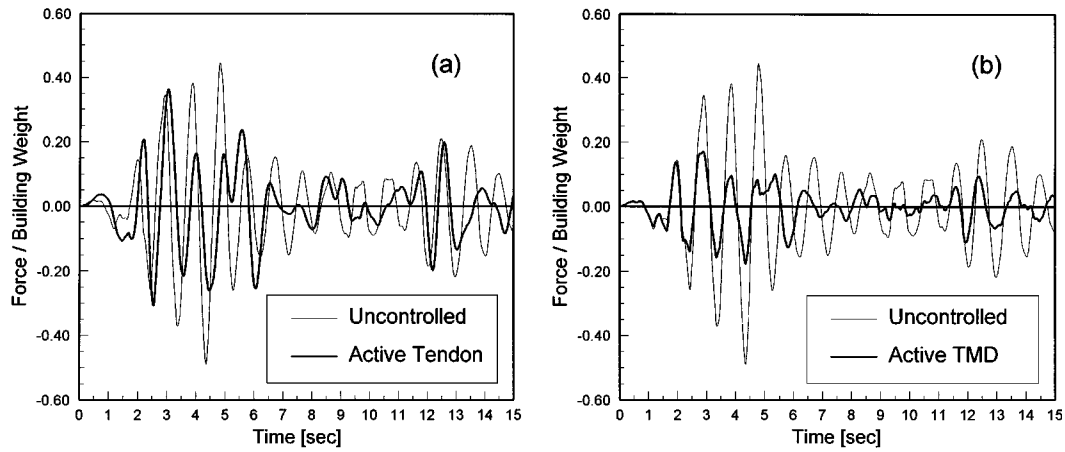

Figure 4. Uncontrolled and controlled base shear: (a) active tendon control and (b) active tuned mass damper control

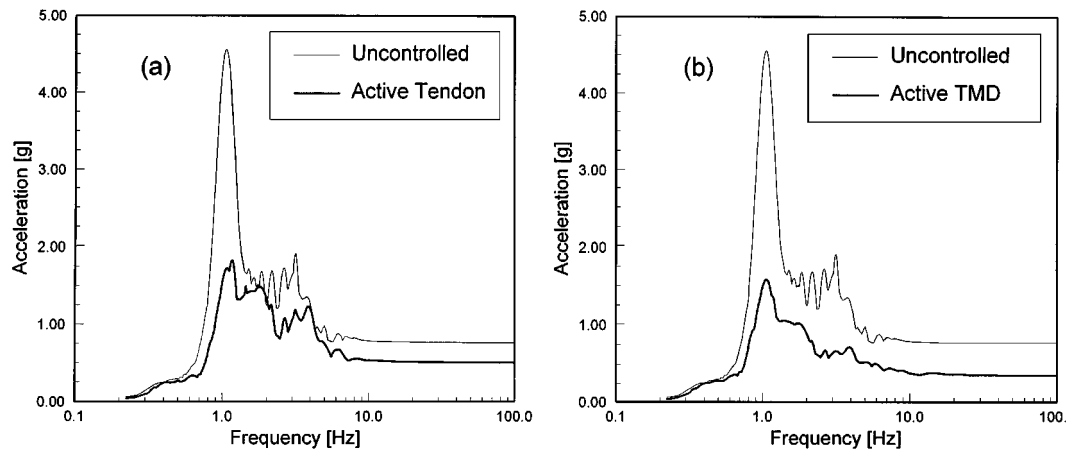

Figure 5. Uncontrolled and controlled floor response spectra for top floor: (a) active tendon control and (b) active tuned mass damper control

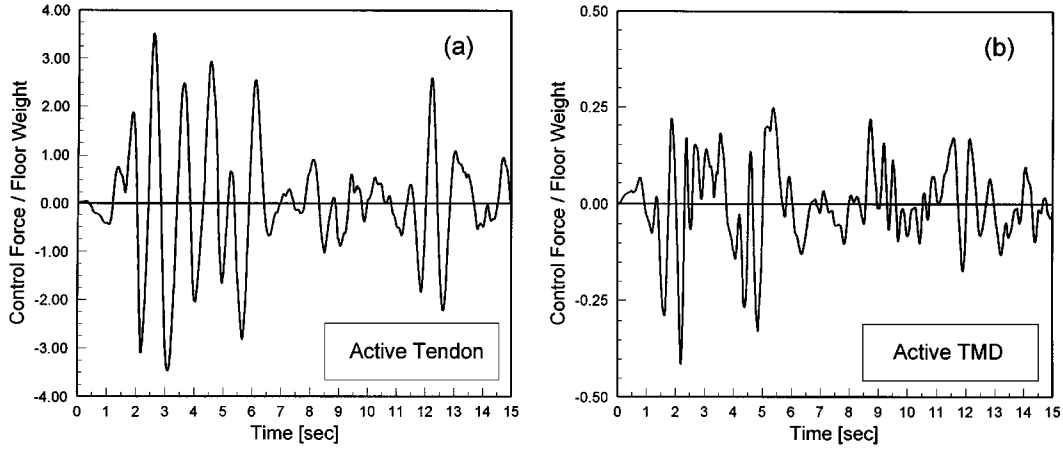

Figure 6. Control force

From the perspective of the practical implementation of any active structural control scheme, the maximum values of the required control force and associated mechanical power (defined as the product of the control force and the velocity of the actuator in the direction of the force) are important operational parameters. These maximum values, in general, depend upon several factors. Intuitively it seems reasonable to think that in a well-designed control algorithm, the control requirements are directly related to the reduction in the response achieved. If a larger reduction is desired then a correspondingly larger level of control force may be required. Unfortunately, in the sliding-mode control approach this relationship between the magnitude of control actions and the level of control achieved is not easy to establish *a priori*. That is, it is not straightforward to regulate the amount of response reduction to a desired predefined level. For a given controller design, the level of control achieved and the corresponding control requirements are determined, to a large extent, by the sliding surface used. For example, if the matrix $\mathbf{C}_{s1}$ is selected by the minimization of a quadratic functional, then the choice of the corresponding weighting matrix $\mathbf{Q}$ determines the sliding surface. The weighting matrix adopted here is a diagonal matrix with the following structure:

$$\mathbf{Q} = \begin{bmatrix} \mathbf{Q}_{11} & \mathbf{0} \\ \mathbf{0} & \mathbf{Q}_{22} \end{bmatrix} \tag{53}$$

The diagonal matrices $\mathbf{Q}_{11}$ and $\mathbf{Q}_{22}$ contain the weights associated with the relative displacements and the relative velocities, respectively. A change in any element of $\mathbf{Q}$ will result into a different sliding surface. For a given controller and for a given input ground motion, once a sliding surface is fixed, it determines the time history of the required control force.

It is not quite clear *a priori* which elements of $\mathbf{Q}$ predominantly govern the relationship between the level of control action and the magnitude of reduction in the response. However, for force actuation through a tuned mass damper, the weighting element affecting the damper's velocity intuitively appears to be the relevant parameter. The following numerical results seem to justify this assumption. In Figure 7, we present the numerical results obtained for different sliding surfaces generated by changing the values of the TMD velocity weighting parameter, ρ_1. This parameter appears in the last element of the matrix $\mathbf{Q}_{22}$. For these results, the elements of $\mathbf{Q}_{11}$ and $\mathbf{Q}_{22}$ are as follows:

$$\mathbf{Q}_{11} = \text{diag}(1000, 1000, 1000, 1000, 1000, 1000, 1000, 1000, 1000, 1500, 50) \tag{54}$$

$$\mathbf{Q}_{22} = \text{diag}(100, 100, 100, 100, 100, 100, 100, 100, 100, 150, \rho_1) \tag{55}$$

In Figure 7(a), we plot the response reduction factors corresponding to the top floor displacements, top floor acceleration and base shear, versus the parameter ρ_1. The response reduction factor is defined as the

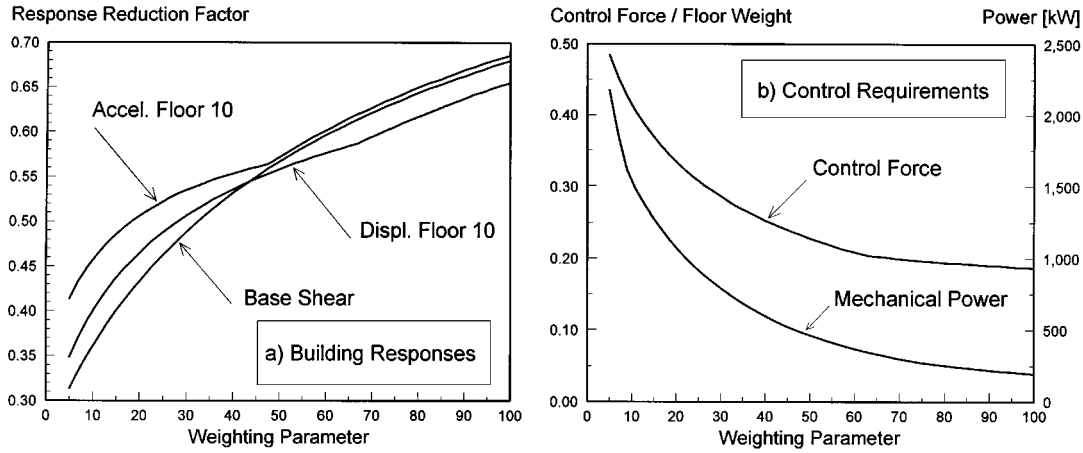

Figure 7. Building responses and control requirements as a function of the parameter defining the sliding surface—active tuned mass damper

ratio between the controlled and uncontrolled maximum values of a given response quantity. A response reduction factor value less than 1·0 indicates that the control scheme is effective in reducing the response; the smaller the value, the more effective the control scheme. In Figure 7(b) we plot the corresponding values of the normalized maximum control force (normalized by a floor-weight) and associated maximum mechanical power, again versus the parameter ρ_1. It is noted that as the parameter ρ_1 is increased, we obtain a smaller reduction in the response, and correspondingly smaller control authority requirements. It is relevant to mention that it was not possible to obtain such relationship between the response reduction and control requirements by arbitrarily changing other parameters of the weighting matrix $\mathbf{Q}$.

Results similar to those presented in Figure 7 are presented in Figure 8 for the control force applied through the active tendon system. Here the parameter which produced desirable relationships between the response reduction and control requirements was the weighting element ρ_2 associated with the displacement of the floor where the tendon forces are applied. The elements of the weighting matrix for this case are as follows:

$$\mathbf{Q}_{11} = 1000\,\mathrm{diag}(\rho_2,\ 1,\ 1,\ 1,\ 1,\ 1,\ 1,\ 1,\ 1,\ 1) \tag{56}$$

$$\mathbf{Q}_{22} = \mathrm{diag}(60,\ 1,\ 1,\ 1,\ 1,\ 1,\ 1,\ 60,\ 300,\ 300) \tag{57}$$

The relationship between control requirements and response reduction factors here is similar to that in Figure 7, except for the response quantity of base shear which is seen to decrease with decreasing control action requirements. It is so because of the fact that this particular response quantity is directly affected by the applied control force and corresponding first floor displacement. A reduced control force applied to the first floor also translates into a reduced base shear value. In Figure 8, we also show the results for the shear in the second storey, which is clearly seen to follow the same general trend as the top floor acceleration and displacement.

For design purposes, it is desirable to have information such as that shown in Figures 7 and 8 whereby one can assess the magnitude of peak force that may be necessary to achieve a particular reduction in the response. In this study, these figures were developed based on rather intuitive arguments and may not correspond with the most optimum choice of the sliding surface. That is, it may be quite possible to obtain better response reduction than shown in these figures for a given level of control effort or obtain a smaller level of control effort for a given reduction in the response. Optimum selection of a sliding surface to obtain a predefined level of performance with a minimum level of control action is a challenging topic for future research.

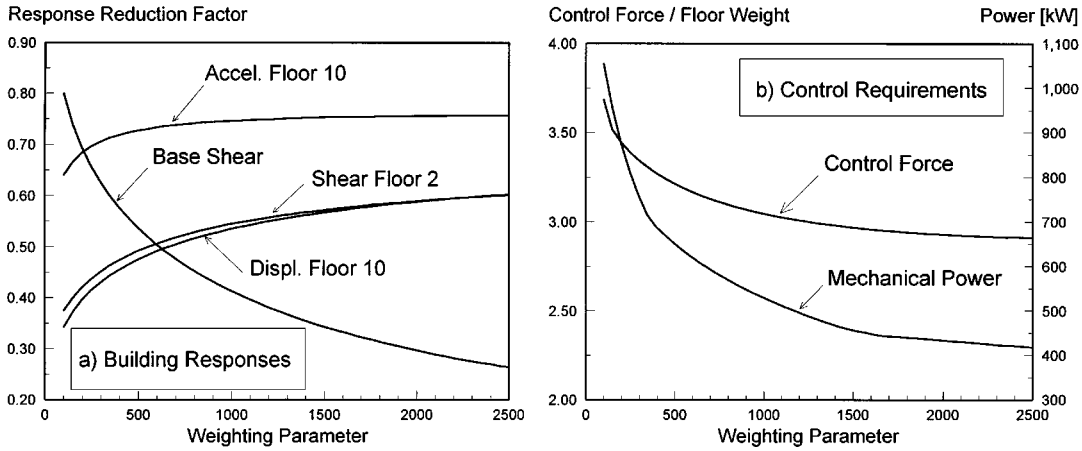

Figure 8. Building responses and control requirements as a function of the parameter defining the sliding surface—active tendon

In the previous set of results only the response of a single floor or a single storey, obtained only for a single seismic input were compared. In the following, we present the controlled response of all building floors, obtained for different seismic inputs.

Table I shows the uncontrolled and controlled displacement response results for the tuned mass damper and active tendon systems for each of the four seismic inputs. The weighting parameters used for the design of the sliding surface were $\rho_1 = 10$ for the tuned mass damper system and $\rho_2 = 150$ for the active tendon system. For each seismic input, the results in the first set of columns (that is, columns (2), (7), (12) and (17)) are the uncontrolled response values of different floors with no control devices installed. The results in the next three columns are the response reduction factors for the tuned mass damper whereas those in the last column under each earthquake are the response reduction factors for the active tendon system. For the tuned mass damper, the results in columns (3), (8), (13) and (18) are for only the tuned mass damper without any active control force. They indicate the effectiveness of the TMD as a passive device. This effectiveness varies with the seismic input. The tuned mass damper as a passive device, is seen to be most effective with El Centro motion and the least with the Loma Prieta motion. The results in the next column sets (that is, columns (4), (9), (14), and (19) are for the active TMD (that is, with active control force). These results, therefore, indicate the combined effect of active and passive control. The ratio of the values in these columns to the ones in the preceding columns are shown in the next set of columns (columns (5), (10), (15) and (20)). These values indicate that application of control force through a tuned mass damper can be effectively used to control the response. This effectiveness is, however, seen to depend on the seismic input. For the example problem considered, the device is most effective with the El Centro earthquake and least effective in the Loma Prieta case with regard to the response of the upper floors and also in the San Fernando case with regard to the displacement responses of the lower floors. The results in the last column set (that is, columns (6), (11), (16), and 21)) are for the active tendon system. It is noted that active tendon systems can also be used for controlling the response.

The results presented in Table II are parallel to those in Table I, but for the acceleration response of various floors. It is noted that the control is not as effective in reducing the acceleration response as it is in reducing the displacement response. In fact, in some instances, especially with the active tendon system, there is some increase in the accelerations of some lower floors. Perhaps the effectiveness of control scheme to reduce the acceleration response can be increased if the minimization functional used to define the sliding surface also includes the acceleration values.

In Table III, we now compare the maximum values of the control force for both methods of force application and for different earthquakes. The first part of the table is for the tuned mass damper and the second part for the active tendon system. For each system, case (a) pertains to lower level of reduction in the response and case (b) for a higher reduction in the response. The response reduction factor values for the top

Table I. Maximum relative displacements

Floor	El Centro					San Fernando					Loma Prieta					Hollywood				
	Response	Resp. red. factor				Response	Resp. red. factor				Response	Resp. red. factor				Response	Resp. red. factor			
		TMD			ATS		TMD			ATS		TMD			ATS		TMD			ATS
	(cm)	Passive	Active	(4)/(3)	Active	(cm)	Passive	Active	(9)/(8)	Active	(cm)	Passive	Active	(14)/(13)	Active	(cm)	Passive	Active	(19)/(18)	Active
(1)	(2)	(3)	(4)	(5)	(6)	(7)	(8)	(9)	(10)	(11)	(12)	(13)	(14)	(15)	(16)	(17)	(18)	(19)	(20)	(21)
10	16·25	0·64	0·40	0·63	0·40	8·92	0·73	0·51	0·70	0·51	6·17	0·98	0·78	0·80	0·90	23·91	0·76	0·46	0·60	0·41
9	15·87	0·63	0·39	0·62	0·40	8·68	0·72	0·53	0·73	0·51	5·96	0·98	0·80	0·82	0·90	23·37	0·76	0·46	0·60	0·41
8	15·14	0·63	0·39	0·62	0·40	8·21	0·73	0·55	0·76	0·51	5·74	0·95	0·81	0·84	0·87	22·30	0·76	0·45	0·60	0·40
7	14·13	0·63	0·39	0·62	0·39	7·53	0·73	0·58	0·79	0·51	5·53	0·93	0·79	0·85	0·80	20·72	0·75	0·46	0·60	0·40
6	12·90	0·62	0·38	0·61	0·38	6·69	0·75	0·60	0·81	0·51	5·23	0·94	0·76	0·81	0·72	18·66	0·75	0·46	0·61	0·40
5	11·36	0·61	0·37	0·60	0·38	5·71	0·77	0·63	0·82	0·51	4·78	0·94	0·73	0·77	0·65	16·17	0·75	0·46	0·61	0·40
4	9·54	0·61	0·36	0·59	0·38	4·70	0·79	0·65	0·82	0·50	4·14	0·95	0·70	0·74	0·62	13·31	0·75	0·46	0·62	0·40
3	7·45	0·61	0·35	0·58	0·41	3·68	0·79	0·65	0·82	0·45	3·29	0·95	0·68	0·72	0·57	10·17	0·75	0·46	0·62	0·40
2	5·13	0·61	0·36	0·59	0·46	2·56	0·79	0·64	0·81	0·46	2·27	0·96	0·67	0·70	0·57	6·84	0·75	0·47	0·63	0·47
1	2·63	0·61	0·36	0·59	0·74	1·32	0·79	0·63	0·80	0·78	1·15	0·96	0·67	0·70	0·98	3·42	0·75	0·48	0·63	0·79

Table II. Maximum absolute accelerations

Floor	El Centro					San Fernando					Loma Prieta					Hollywood				
	Response	Resp. red. factor				Response	Resp. red. factor				Response	Resp. red. factor				Response	Resp. red. factor			
		TMD			ATS		TMD			ATS		TMD			ATS		TMD			ATS
	(g)	Passive	Active	(4)/(3)	Active	(g)	Passive	Active	(9)/(8)	Active	(g)	Passive	Active	(14)/(13)	Active	(g)	Passive	Active	(19)/(18)	Active
(1)	(2)	(3)	(4)	(5)	(6)	(7)	(8)	(9)	(10)	(11)	(12)	(13)	(14)	(15)	(16)	(17)	(18)	(19)	(20)	(21)
10	0·76	0·67	0·46	0·68	0·67	0·48	0·97	0·57	0·59	0·82	0·49	0·92	0·53	0·57	0·81	1·03	0·78	0·45	0·58	0·59
9	0·72	0·68	0·46	0·68	0·64	0·44	0·95	0·56	0·59	0·79	0·42	0·92	0·64	0·70	0·87	1·01	0·76	0·46	0·61	0·56
8	0·64	0·70	0·48	0·69	0·61	0·39	0·86	0·70	0·81	0·67	0·33	0·98	0·83	0·85	0·95	0·96	0·75	0·47	0·63	0·50
7	0·60	0·66	0·54	0·82	0·53	0·35	0·80	0·85	1·07	0·67	0·28	0·95	0·96	1·01	0·86	0·90	0·73	0·49	0·67	0·44
6	0·58	0·57	0·53	0·93	0·45	0·35	0·83	0·88	1·07	0·75	0·36	0·97	0·71	0·73	0·85	0·82	0·71	0·51	0·72	0·43
5	0·54	0·66	0·52	0·78	0·53	0·41	0·87	0·72	0·83	0·69	0·42	0·98	0·60	0·61	0·85	0·72	0·67	0·53	0·79	0·44
4	0·50	0·69	0·51	0·74	0·58	0·43	0·90	0·66	0·73	0·71	0·43	0·98	0·54	0·55	0·81	0·64	0·69	0·55	0·81	0·45
3	0·44	0·70	0·56	0·80	0·59	0·37	0·91	0·72	0·79	0·70	0·37	0·99	0·61	0·61	0·75	0·55	0·73	0·60	0·83	0·53
2	0·35	0·75	0·70	0·93	0·78	0·33	0·96	0·82	0·85	0·82	0·28	1·00	0·89	0·89	1·09	0·44	0·80	0·69	0·87	0·59
1	0·26	0·91	1·03	1·13	1·41	0·31	0·98	0·90	0·92	1·14	0·29	1·00	0·94	0·95	1·28	0·32	0·95	0·85	0·89	0·86

Table III. Maximum control force requirements

	Tuned mass damper				Active tendon system			
	Case a		Case b		Case a		Case b	
	Resp. red. factor	Max. control force (Floor weight)	Resp. red. factor	Max. control force (Floor weight)	Resp. red. factor	Max. control force (Floor weight)	Resp. red. factor	Max. control force (Floor weight)
	(1)	(2)	(3)	(4)	(5)	(6)	(7)	(8)
El Centro	0·59	0·20	0·40	0·42	0·59	2·92	0·40	3·52
San Fernando	0·69	0·13	0·51	0·28	0·76	2·38	0·51	2·39
Loma Prieta	0·92	0·16	0·78	0·40	0·96	2·49	0·90	2·65
Hollywood	0·70	0·19	0·46	0·38	0·60	4·85	0·41	5·36

Table IV. Maximum storey shears

Floor	El Centro					San Fernando					Loma Prieta					Hollywood				
	Response	Resp. red. factor				Response	Resp. red. factor				Response	Resp. red. factor				Response	Resp. red. factor			
		Passive devices			Semi-active		Passive devices			Semi-active		Pasive devices			Semi-active		Passive devices			Semi-active
	(Bldg weight)	Stiff-ness	Damp-ing	Stiffness damping		(Bldg weight)	Stiff-ness	Damp-ing	Stiffness damping		(Bldg weight)	Stiff-ness	Damp-ing	Stiffness damping		(Bldg weight)	Stiff-ness	Damp-ing	Stiffness damping	
(1)	(2)	(3)	(4)	(5)	(6)	(7)	(8)	(9)	(10)	(11)	(12)	(13)	(14)	(15)	(16)	(17)	(18)	(19)	(20)	(21)
10	0·08	1·22	0·93	1·12	0·90	0·05	1·20	0·97	1·15	0·96	0·05	1·18	0·91	1·09	0·99	0·10	1·10	0·91	1·04	0·93
9	0·15	1·11	0·93	1·02	0·82	0·09	1·09	0·98	1·04	0·91	0·09	1·05	0·91	0·97	0·93	0·20	0·99	0·91	0·94	0·83
8	0·21	1·03	0·93	0·94	0·75	0·13	0·97	0·98	0·94	0·85	0·12	0·96	0·92	0·90	0·90	0·30	0·90	0·91	0·85	0·75
7	0·27	0·97	0·93	0·88	0·68	0·16	0·87	0·98	0·85	0·79	0·14	0·90	0·97	0·87	0·89	0·39	0·81	0·90	0·77	0·68
6	0·31	0·99	0·93	0·90	0·67	0·18	0·86	0·97	0·85	0·78	0·15	0·91	0·97	0·89	0·89	0·47	0·80	0·90	0·76	0·66
5	0·36	0·98	0·93	0·90	0·64	0·20	0·89	0·96	0·87	0·80	0·16	0·95	0·98	0·93	0·90	0·53	0·79	0·90	0·75	0·65
4	0·40	0·97	0·92	0·89	0·61	0·22	0·95	0·96	0·92	0·84	0·17	1·03	0·97	1·00	0·93	0·59	0·78	0·89	0·75	0·64
3	0·44	0·95	0·93	0·87	0·58	0·22	1·02	0·95	0·99	0·88	0·19	1·02	0·97	0·99	0·92	0·62	0·78	0·89	0·75	0·64
2	0·47	0·92	0·94	0·84	0·55	0·23	1·01	0·94	0·97	0·86	0·21	1·04	0·96	1·01	0·93	0·64	0·79	0·90	0·75	0·64
1	0·49	0·90	0·94	0·82	0·54	0·25	0·94	0·93	0·91	0·79	0·21	1·08	0·96	1·04	0·95	0·64	0·80	0·93	0·76	0·65

floor displacement response are shown in columns (1) and (5) for case (a) and in columns (3) and (7) for case (b). The lower this value, the higher is the reduction in the response. The corresponding maximum control forces are given in columns (2) and (6) for case (a) and in columns (4) and (8) for case (b), respectively. These values are presented as the ratio of the control force to the floor weight.

We note that control force values are the smallest for the tuned mass damper system and the highest for the active tendon system. The force required in the active tendon system, being large, may not be practically feasible. We also note that different seismic inputs demand different levels of the force. For the example problem considered here, we note that for the Kern County Hollywood earthquake, the maximum force required is about five times the floor weight. At a level for 0·3 g, this earthquake has significantly more energy at the predominant frequency of the structure, as is seen from its ground response spectrum value in Figure 2, thus demanding a larger control action for comparable response reduction.

3.2. Semi-active control

The results presented in the previous section indicate that active control can, indeed, reduce a structure's response, but the magnitude of the control requirements can be quite high. As such, alternative methods of controlling structures are being sought. One promising approach which has attracted attention of researchers is the semi-active control approach. In this approach no significant external energy is input into the structure, as it is the case with the active control scheme. One appropriately regulates structural parameters to achieve desirable results such as a reduction of dynamic response. Such parametric regulation can be performed for example by controlling valve opening and closing for stiffness and damping change or by changing the viscosity of a damper fluid for damping coefficient change. Such operations may require only a nominal amount of external power. This has led to research on the application of electrorheological and magnetorheological dampers for seismic response control.

In the following, we investigate the effectiveness of semi-active devices operated accordingly to the sliding-mode control approach. Here, we have considered a somewhat idealized situation where we can change the damping and stiffness matrices of the structure independently by turning on or off the stiffness and damping elements provided in the diagonal bracings of a structure. Therefore, the regulation of the semi-active devices is done according to equations (50) and (51), with $k_{v_i}^{\min} = 0$ and $c_{v_i}^{\min} = 0$.

We first present the numerical results for semi-active control through damping regulation. For this set of results, supplementary on–off viscous dampers are installed in the first nine storeys. The maximum damping coefficient for the devices in the first seven storeys is 1·75 c_{ref}, with $c_{\text{ref}} = 6{\cdot}15$ (MNs/m). The damping coefficients for the devices in the eighth and ninth storeys are 1·05 c_{ref} and 0·70 c_{ref}, respectively. This distribution of damping in different stories has been arbitrarily selected. If these additional dampers are left on all the time, the first mode damping ratio is increased from a value of 3·1 per cent to about 5·2 per cent of the critical.

The responses of the controlled and uncontrolled systems are compared in Figures 9(a) and 9(b), in which we show the time histories of the top floor displacement and the base shear force, respectively, for El Centro ground motion. It is noted that the supplementary damping devices are effective in reducing both responses.

The introduction of any additional damping in a building structure, whether it is changed or not, will lead to some dissipation of vibration energy and thus an overall reduction in the response. The question then is, does the regulation of the dampers, according to (51), improve the performance of the system when compared to the case in which the dampers operate in a full passive mode?

To investigate this, the numerical results presented in Figure 10 were obtained. In this figure, we compare various floor and storey responses for the two cases of passive and semi-active dampers. The response reduction factors for relative displacement, acceleration and shear force responses corresponding to the fully passive case are less that 1·0 and they indicate the increased ability of the system to dissipate energy. However, the response reduction factors associated with switching of the damping devices show that semi-active control did not reduce the response any further in this particular case.

The effect of the magnitude of the supplementary damper coefficient on the semi-active performance was numerically investigated and several sets of results were obtained. Even when damper coefficients as large as

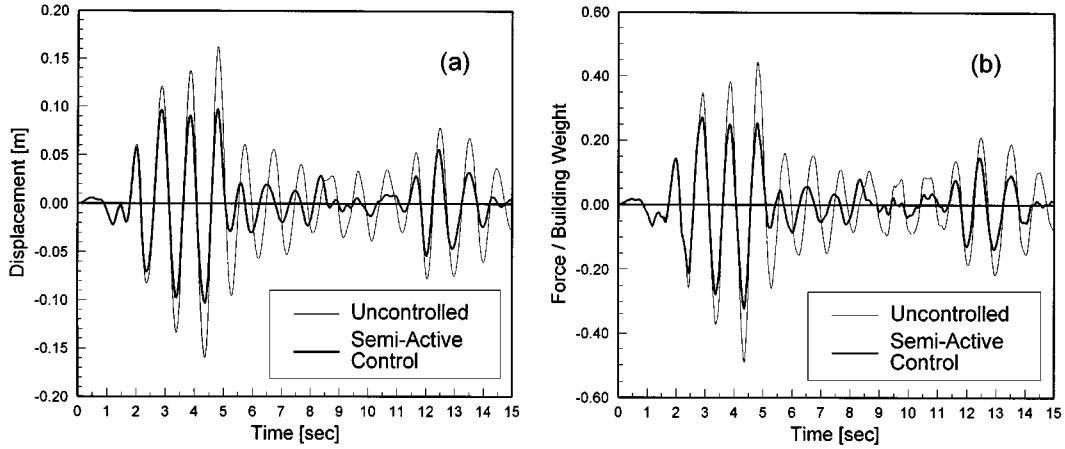

Figure 9. Uncontrolled and controlled responses—semi-active damping control: (a) top floor displacement and (b) base shear

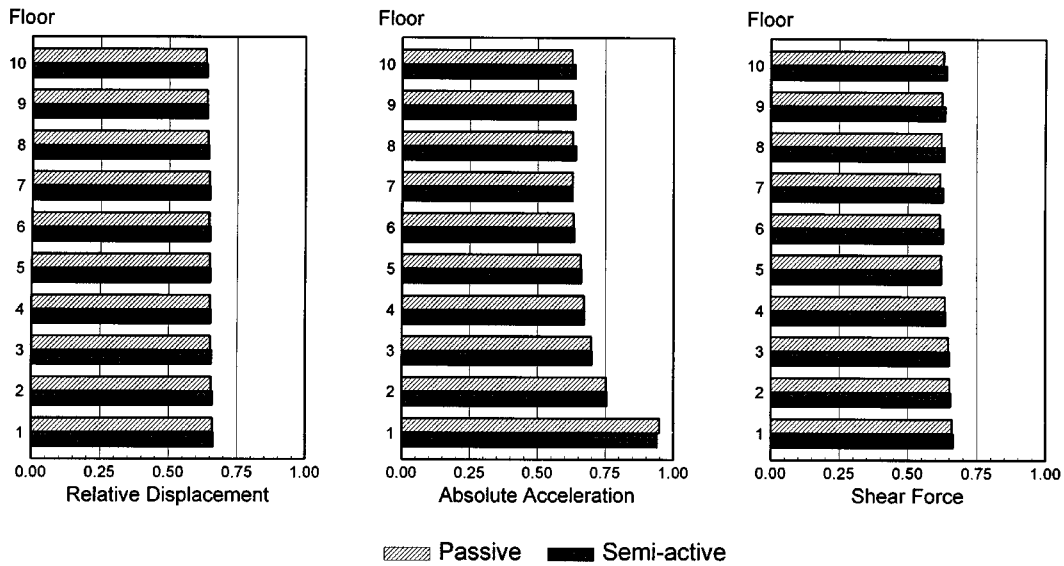

Figure 10. Comparison of response reduction factors for passive and semi-active damping control

to generate a maximum damping force equal to 75 per cent of the floor weight were used, the semi-active operation did not produce any significantly smaller responses than those obtained when the dampers were left on all the time. We must underline the fact that these conclusion have been established by comparing passive dampers with damping coefficient $c_{v_i}^{max}$ and semi-active dampers with two-state damping coefficients $(0, c_{v_i}^{max})$. That is, in the passive case the dampers are assigned a constant damping coefficient equal to the upper limit for the dampers in the semi-active case.

Since the results obtained here depend upon the choice of a sliding surface used, theoretically it may still be possible to get better results with switchable damping perhaps with another more optimum sliding surface, specifically adapted to the characteristics of the semi-active damping control operation. However, the results presented here indicate that linear viscous dampers are quite effective as passive devices, but their active regulation may not be significantly beneficial for the type of structural systems. Nonetheless, semi-active

control systems based on damping regulation may be quite effective for other structural systems. A typical example is found in vehicle suspension systems. In this case, high values of damping may adversely affect the performance of the isolation system and the determination of the optimal amount of damping is a crucial problem. For these systems, semi-active dampers may provide an effective way to improve the isolation characteristics.[27] Another example is found in bridge structures, for which hybrid vibration isolation systems consisting of rubber bearings and variable dampers have been proposed as an effective way to reduce seismic responses.[10]

Finally, we present the numerical results for semi-active stiffness control. For this, the structure is equipped with switchable bracings, which can be attached and detached in the first nine storeys. The first seven storeys have devices which provide additional stiffness up to 30 per cent of the storey stiffness when they are attached. The bracings in the eighth and ninth storeys provide up to 20 and 10 per cent of the storey stiffnesses, respectively. The tenth storey does not have any additional bracings. In addition to the stiffness, the bracings also have damping elements which provide additional damping up to about 0·25 c_{ref}.

Figures 11(a) and 11(b) show the uncontrolled and semi-active controlled response time histories of the top floor displacement and base shear for the El Centro ground motion. The effectiveness of the semi-active control is clearly seen from these plots.

In Figure 12, we investigate the control effectiveness in terms of the reduction it brings about in various floor and storey responses. From the figure we note that a mere addition of stiffness passively can increase some response quantities; it depends on where the structure's dominant frequencies are situated with respect to the input motion response spectrum. In the case of this particular building, the addition of stiffness puts the structure in the higher acceleration response spectrum range. As a result, the acceleration response of the higher floors are increased. Also increased are the shear forces in the higher storeys. On the other hand, the semi-active operation of the supplemental stiffness clearly reduces most of the response quantities. It is noticed that the displacement and interstorey shear responses are significantly reduced for all floors. However, the reduction in the acceleration response is not as significant; in fact, for the first floor the acceleration response is slightly increased.

Figure 13(a) shows the time history for the control force generated by the semi-active device installed in the first storey. To show the dissipation of energy caused by active regulation of the stiffness, Figure 13(b) shows, for the same device, the control force versus the corresponding storey drift. The formation of hysteresis loops due to semi-active stiffness control is clearly seen from this figure.

To compare the effectiveness of semi-active stiffness control for different seismic inputs, we present the results of Table IV for storey shear responses. For each earthquake input, the results in the first set of columns (nos. 2, 7, 12, and 17) are the uncontrolled response values, whereas the values presented in columns

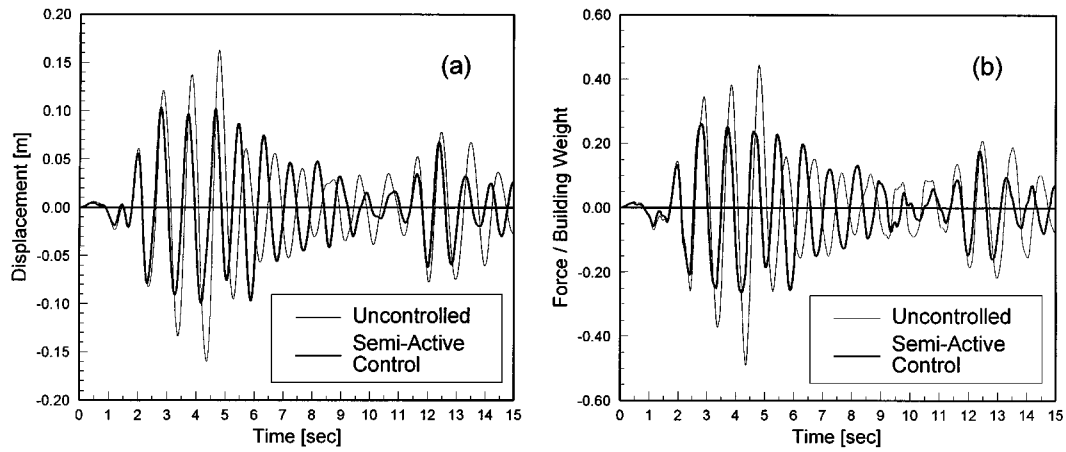

Figure 11. Uncontrolled and controlled responses—semi-active stiffness control: (a) top floor displacement and (b) base shear

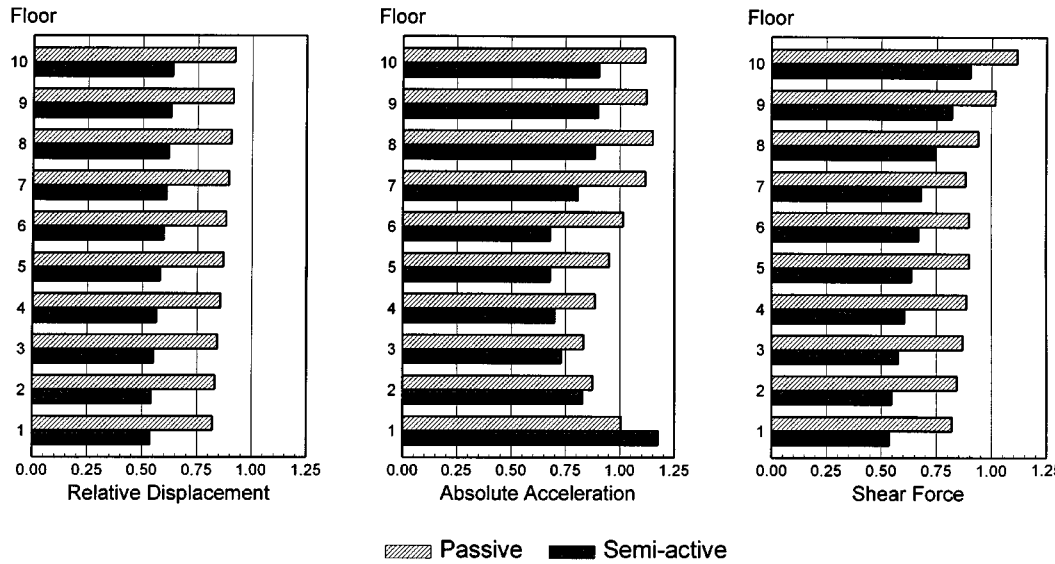

Figure 12. Comparison of response reduction factors for passive and semi-active stiffness control

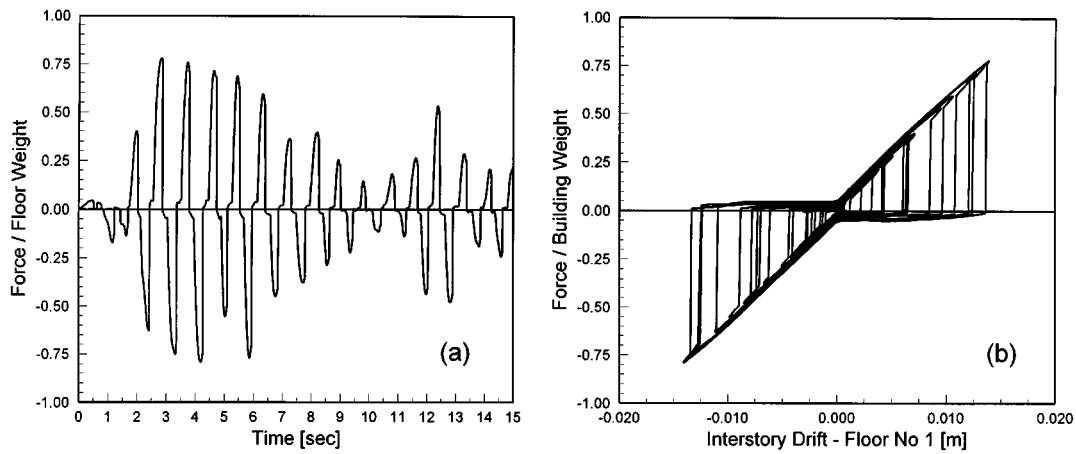

Figure 13. Semi-active stiffness control: control force—floor no 1

(3), (8), (13) and (18) represent the response reduction factors when the structure is passively stiffened. It is seen that shear force is significantly increased especially in the top storeys of the structure by a passive stiffening of the structure. The results in the next column sets (nos. 4, 9, 14, and 19) are for only the supplementary damping elements acting passively. In this case all storey shear values are decreased, with a slightly larger reduction in the top storeys than in the bottom stories. When both the stiffness and damping elements are installed and act passively, the damping elements tend to compensate the increase caused by the passive stiffening. These results are shown in columns (5), (10), (15) and (20). In the next set of columns we show the results when the stiffness elements are actively regulated. The final reduction in the response caused by semi-active stiffness control is quite evident. The approach seems to be most effective on the El Centro motion and least on the Loma Prieta motion. This suggests that perhaps an adaptive sliding-mode control approach, which adapts the sliding surface to the special characteristics of each input motion is likely to perform better.

4. CONCLUSIONS

The application of sliding-mode control for active and semi-active control of civil structures is investigated. A new formulation, based on the singular value decomposition of the input matrix, is presented to transform the system equations into their regular form and to obtain the description of the sliding motion for the case of control redundancy.

A 10-storey building with mass and frequency characteristics similar to those found in practice is chosen so that the practical feasibility of the required control actions can be ascertained. To examine the variability of control effectiveness to different seismic inputs, four recorded ground motions are considered as input disturbances.

The numerical results for the active control indicate that, if the required control force can be provided, active control schemes can be quite effective in reducing the seismically induced responses. This effectiveness was observed to vary with the seismic input considered. With respect to the control requirements, it was observed that the peak control force in the active tendon system was much larger than that required in the tuned mass damper system. The force required in the tuned mass damper system seems to be reasonable but it is associated with high velocities of the auxiliary mass.

In the application of semi-active control schemes, it was observed that the passive installation of supplementary linear viscous damping devices reduced the structural response by merely cyclic dissipation of energy, but their active regulation did not produce any larger reductions, at least for the structural applications considered in this study. The switching of supplementary stiffness elements was, however, found to be useful in reducing the structural response. It is observed that stiffness switching produces triangular shaped hysteresis loops representing a dissipation of energy.

ACKNOWLEDGEMENTS

This research is sponsored by the National Science Foundation through Grant No. BCS-9301574. This support is gratefully acknowledged.

REFERENCES

1. U. Itkis, *Control Systems of Variable Structure*, Wiley, New York, 1976.
2. V. I. Utkin, *Sliding Modes and their Application in Variable Structure Systems*, Mir Publishers, Moscow, 1978.
3. V. I. Utkin, *Sliding Modes in Control and Optimization*, Springer, Berlin, 1992.
4. K. D. Young, 'Design of variable structure model following systems', *IEEE trans. automat. control* **23**, 1079–1085 (1978).
5. J. J. Slotine and S. S. Sastry, 'Tracking control of nonlinear systems using sliding surfaces, with application to robor manipulators', *Int. j. control* **38**, 465–492 (1983).
6. H. Sira-Ramirez, 'Variable structure control of nonlinear systems', *Int. j. systems sci.* **18**, 1673–1689 (1987).
7. R. A. DeCarlo, S. H. Zak and G. P. Matthews, 'Variable structure control of nonlinear multivariable systems: A tutorial', *Proc. IEEE* **76**, 212–232 (1988).
8. J. N. Yang, Z. Li, J. C. Wu and K. D. Young, 'A discontinuous control method for civil engineering structures', in L. Meirovitch (ed.), *Proc. 9th VPI&SU symp. on dynamics and control of large structures*, Blacksburg, VA, (1993) pp. 167–180.
9. J. N. Yang, J. C. Wu, A. K. Agrawal and Z. Li, 'Sliding mode control for seismic-excited linear and nonlinear civil engineering structures', *Technical Report NCEER-94-0017*, National Center for Earthquake Engineering Research, 1994.
10. J. N. Yang, J. C. Wu, K. Kawashima and S. Unjoh, 'Hybrid control of seismic-excited bridge structures', *Earthquake eng. Struct. Dyn.* **24**, 1437–1451 (1995).
11. J. N. Yang, J. C. Wu and A. K. Agrawal, 'Sliding mode control of seismic-excited linear structures', *J. Eng. Mech.* **121**, 1330–1339 (1995).
12. J. N. Yang, J. C. Wu and A. K. Agrawal, 'Sliding mode control of nonlinear and hysteretic structure', *J. Eng. Mech.* **121**, 1386–1390 (1995).
13. J. N. Yang, J. C. Wu, A. M. Reinhorn and M. Riley, 'Control of sliding-isolated buildings using sliding mode control', *J. struct. eng.* **122**, 179–186 (1996).
14. M. P. Singh and E. E. Matheu, 'Hybrid sliding mode control of civil structures', in L. Meirovitch (ed.), *Proc. 10th VPI&SU symp. on dynamics and control of large structures*, Blacksburg, VA, 1995, pp. 323–334.
15. A. G. Lukyanov and V. I. Utkin, 'Methods of reducing equations for dynamic systems to a regular form', *Automat. remote control* **4**, 5–13 (1981).
16. V. N. Brandin and G. N. Razorenov, 'Decoupling of nonlinear systems', *Automat. remote control* **10**, 5–11 (1979).
17. C. M. Dorling and A. Zinober, 'Two approaches to hyperplane design in multivariable variable structure control systems', *Int. j. control* **44**, 65–82 (1986).
18. V. I. Utkin, 'Equations of the sliding regime in discontinuous systems—Part I', *Automat. Remote Control* **12**, 42–54 (1971).
19. V. I. Utkin and K. D. Young, 'Methods for constructing discontinuous planes in multidimensional variable structure systems', *Automat. Remote Control* **31**, 1466–1470 (1978).

20. C. M. Dorling and A. Zinober, 'Robust hyperplane design in multivariable variable structure control systems', *Int. j control* **48**, 2043–2054 (1988).
21. G. Ambrosino, C. Celentano and F. Garofalo, 'Variable structure model reference adaptive control systems', *Int. j. control* **39**, 1339–1349 (1984).
22. J. A. Burton and A. Zinober, 'Continuous approximation of variable structure control', *Int. j systems sci.* **17** (6), 875–885 (1986).
23. G. Leitmann, 'Guaranteed asymptotic stability for some linear systems with bounded disturbances', *ASME j. dyn. systems meas. control* **23**, 1079–1085 (1978).
24. M. Corless and G. Leitmann, 'Continuous state feedback guaranteeing uniform ultimate boundedness for uncertain dynamic systems', *IEEE trans. automat. control* **26**, 1139–1144 (1981).
25. E. P. Ryan and M. Corless, 'Ultimate boundedness and asymptotic stability of a class of uncertain dynamical systems via continuous and discontinuous feedback control', *IMA j. math. control optim.* **1**, 223–242 (1984).
26. F. Zhou and D. G. Fisher, 'Continuous sliding mode control', *Int. j. control* **55**, 313–327 (1992).
27. D. Karnopp, 'Design principles for vibration control systems using semi-active dampers', *ASME j. dyn systems, meas. control* **112**, 448–445 (1990).